Methanolysis of Africa pear seed oil via thermally activated empty palm fruit bunch ash (TAEPFBA) catalyst. ANN prediction and sensitivity analysis

Comment [h1]: The total words should be reframed, not longer than 18 words

Abstract

This study investigated the catalytic effect of thermal modified empty palm fruit bunch ash (TAEPFBA) on the transesterification reaction of Africa pear seed oil (APSO) with optimization of the process and relative contribution. The TAEPFBA was synthesized from empty palm fruit bunches while the APSO was extracted via solvent extraction. The oil and catalyst were characterized using America Society for Testing Material (ASTM) and analytical tools. The transesterification reaction was optimized and predicted with artificial neural network (ANN). The methyl ester produced was characterized and compared with standard properties for its application. The results showed that the oil and catalyst had comparable properties with other oils and catalysts that have been used for transesterification. The optimal conditions for transesterification reaction are temperature of 60^{o}C, reaction time of 3hrs, 10:1 methanol/oil molar ratio, 3wt catalyst dosage and agitation speed of 300rpm with biodiesel yield of 75%. The biodiesel produced was within the acceptable standard. The ANN accurately predicted the yield of biodiesel with a mean square error (MSE) value of .0214. The contributive impact of each process variable shows that the temperature has the highest relative impact on the yield of biodiesel while the methanol/oil molar ratio has the least contribution Therefore, the catalyst (TAEPFBA) has the potential to convert the APSO to alkyl ester and the yield can be predicted with ANN tool.

Comment [h2]: REPHRASE WITH….optimized transesterification reaction of African pear seed oil (APSO) with relative contribution of process factors

Comment [h3]: REPHRASE WITH: and Association of Officials of analytical Chemists (AOAC) methods

Comment [h4]: fatty methyl ester

Comment [h5]: ASTM standards

Comment [h6]: delete

Comment [h7]: REPLACE WITH: suitable

Comment [h8]: were

Comment [h9]: 3 wt.%

***Keywords**: Africa pear seed oil, thermal activated empty palm fruit bunch ash (TAEPFBA), biodiesel, ANN, and sensitivity analysis*

Comment [h10]: delete

Comment [h11]: REPHRASE WITH: prediction and sensitivity analysis.

Comment [h12]: Replace with: palm fruit ash

Comment [h13]: delete

1.0 Introduction

Biodiesel is considered a replacement for depleting convectional diesel because it is renewable, environmentally friendly, and non-toxic fuel and can be blended with petro-diesel. Biodiesel has remained vital because of its usage in diesel engines to convey heavy loads, which is impossible with other fossil fuels or bio-energy. Moreover, it contains oxygen, which enhances the combustion process in diesel engines and reduces the emission of harmful gases, soot, and unburnt hydrocarbons [1] [2][3]. Hence, it is a potential substitute for petro-diesel [4] [5][6][7]. In the recent past, biodiesel production has promoted economic development in some European countries. Biodiesel is predominantly produced via the transesterification process.

Comment [h14]: [1-3]

Comment [h15]: [1-7]

Transesterification reactions have been carried out with many edible oils such as *cocos nucifera* oil, *elaeis guineensis*, groundnut oil, cashew oil, avocado oil e.t.c. However, the use of these oils to produce biodiesel was discontinued due to how it affects food availability and the cost of living, especially in

Comment [h16]: Replace with: coconut oil

Comment [h17]: Replace with: African oil palm

developing countries. Various non-edible biomass such as castor [8], tamanu [9], rubber seed [10], jatropha curcas [11], neem [12), *pongamia pinnata* [13], *rubber seed* [14], cottonseed [15] etc. have been used to produce biodiesel. Non-edible seed oils of African pear seed oil (APSO) have been gaining the attention of researchers in recent times especially in Nigeria. It is an annual fruit, and contains 49–53% oil per seed, and a plantation can produce 8–9 tonnes of oil per hectare.

The nature of the catalyst determines the percentage conversion of oil (like APSO) to biodiesel. Onukwuli and Ude [16] used activated clay as a catalyst to produce 78%-80% biodiesel from APSO. Iloamaeke *et al.* [17] applied two-step transesterification using H_2SO_4 and NaOH to have 69% APSO conversion to biodiesel. Isong *et al* [18] used NaOH to synthesize biodiesel (87% yield) from *dacryodes edulis* while Bull and George [19] studied the transesterification of biodiesel with NaOH with a percentage yield of 80%. The research on the use of heterogenous catalysts in APSO conversion to biodiesel is limited and this has spurred the research on the use of EPFBA in raw and activated form as a catalyst in the methanolysis of APSO to biodiesel. To the best of my knowledge, there is no report on the percentage of APSO oil converted to bioidiesel using raw and thermally activated empty palm fruit bunch ash (EPFBA). It is relevant to ascertain some vital physiochemical and thermal properties of biodiesel produced with thermal activated EPFBA in order to widen its application in biodiesel technology.

Comment [h18]: delete

Comment [h19]: Replace with: no literature information was found....

The EPFBA is a catalyst synthesized from empty palm fruit bunches (EPFB), which is the most abundant waste found in oil palm mills. Oil palm is one of the most essential edible oils that is readily available with high economic value. It is grown in large quantities in Nigeria. A palm tree harvested and processed could produce waste such as empty palm fruit bunches (EPFB), palm oil mill effluent, and palm kernel shell. This EPFB is considered to be an emerging issue because of its disposal cost and its effect on the drainage system when not used or disposed of properly. The use of the EPFB as a catalyst in biodiesel production could minimize these challenges.

Comment [h20]: delete

Comment [h21]: replace with: was

The EPFBA catalyst and other variables like time, catalyst, alcohol/oil ratio, speed, and temperature affect the biodiesel yield. It is difficult to optimize the process by one factor or two factors at a time approach. Alternatively, response surface methodology (RSM), RSM linked with genetic algorithm (GA), artificial neural network (ANN), and adaptive neural fuzzy interference system (ANFIS) are reliable techniques to

use. Several researchers have identified these techniques as reliable optimization tools. Zabeti *et al.* [20] used response surface methodology to predict the biodiesel yield produced using alumina–supported calcium oxide. Onukwuli *et al.* [17] employed response surface methodology in the optimization of biodiesel production from crude cottonseed oil using sodium hydroxide as a catalyst. Therefore, this study focused on the transesterification of Africa pear seed oil using thermally activated EPFBA, optimization of the process, and the relative contribution of the input variables to the yield.

2. MATERIALS AND METHODS

2.1 Materials

The Africa pear seeds were purchased from Okigwe in Imo State, Nigeria, and the seeds were gathered after the edible parts had been consumed. The empty palm fruit bunch was collected from individuals that have a large oil plantation in Okigwe, Imo State, Nigeria. The reagents were procured from Kelechi Science Laboratory Ltd., Okigwe Market, Imo State, Nigeria, and they were of analytical grade.

Comment [h22]: Include Okigwe coordinates i.e 5.483^{O} N 7.55^{o} E

Comment [h23]: name the reagents

2.2 Methods

2.2.1 Extraction of oil and its characterization

The seeds were dried in sunlight for thirty days, deshelled, and the kernels were milled using a Kenwood electrical grinder KEFP580 prior to oil extraction. Solvent extraction as described by Zahira [21] was adopted in extracting the oil from the seed. The extraction was carried out by using a soxhlet extractor containing the milled kernel (particle size of 900µm), fitted with a round bottom flask (2 L capacity). The extraction was achieved on a water bath for 6 hrs, with n-hexane solvent (Bpt 40-60^{o}C). The oil and n-hexane contained in the beaker are subjected to a temperature above 70^{o}C to vapourize and recover the n-hexane. The percentage mass of oil is determined using Equation 1. The Africa pear seed oil was characterized with ASTM to determine its physiochemical properties.

$$A = \frac{N_o}{N} * 100 \quad . \quad (1)$$

Where, A represent the percentage of oil extracted from the seed

N_o is the mass of pure oil extracted (g)

N is the mass of the seed prior to extraction

2.2.2 Preparation and synthesis of catalyst

The raw empty palm fruit bunch (EPFB) was cut into small pieces and air dried. The dried EPFB was milled using a laboratory blender. The pulverized biomass was sieved through a 250 ụm diameter sieve to get fine particles and submerged in distilled water for 12 hrs. It was decanted to remove impurities, then left to drain before being dried in a hot air oven at 104°C until it reached a consistent weight. The EPFB was then burned for 4 hrs at 800°C in a furnace to produce empty palm fruit ash, or EPFBA. The dried EPFBA was subjected to heat treatment in a muffle furnace until a temperature of 1000^{o}C was reached for 1hr.

2.2.3. Physiochemical properties of catalyst

The properties of the raw and thermally modified EPFBA samples were determined using various analytical instruments. The ASTM D4067 method, and multi-point **Brunauer-Emmet-Teller** BET (Nova station Quantachrome instrument version 11.3) were used to determine their physiochemical properties of the raw and activated EPFBA. The fourier transform infra-red spectrometer (FTIR) transmission method using KBr (BUCK model 500M) was employed to determine the functional group, while a Carl Zeiss sigma field emission scanning electron microscope (SEM) was used to determine the morphology of the EPFBA samples, and the group and the crystallographic structures of the EPFBA were recorded using an X-ray diffractometer (XRD). The x-ray diffraction measurements were performed in a Shimadzu diffractometer model XRD-7000 with Cu Ka X-ray source (40 kV, 30 mA, λ = 1.5418 Å).

2.2.4 Transesterification reaction

The extracted oil from Africa pear seed react with methanol in the presence of raw EPFBA or thermal activated empty palm fruit bunch ash (TAEPFBA) to produce fatty acids methyl ester FAME, and glycerol. The flat bottom flask containing the oil, catalyst (3% weight of oil sample) and methanol (10:1 methanol/oil molar ratio) was placed on a hot magnetic stirrer at a constant temperature with a set agitation speed of 300 rpm during the reaction. The flask was removed after 3 hours, cooled, and the biodiesel in the upper layer was separated from the by-product (glycerol) in the lower layer by overnight settlement at room temperature. The catalyst was recovered by filtration using filter paper, and the excess methanol in the

upper layer was recovered by rotary evaporation. The optimal percentage of biodiesel yield was calculated as shown in Equation 2.

$$\text{Biodiesel (\%)} = \frac{weight\ of\ biodiesel}{weight\ of\ oil\ used} \times 100 \quad (2)$$

2.2.5 Effect of process parameters on biodiesel yield

The effect of process variables on the yield of biodiesel was investigated experimentally. To study the effect of one parameter the other variables are kept constant. The variables considered were catalyst (raw and activated), methanol/oil ratio, temperature, reaction time, and agitation speed.

Comment [h24]: State these combination ratios of the process parameters

2.2.6 Statistical design and optimization approach

The multi-input-single-output (MISO) ANN model in Figure 1 was adopted to model the performance of the input parameters and predict the optimal yield of alkyl ester. The input variables processed in the hidden layers are catalyst, methanol/oil ratio, temperature, reaction time, agitation speed, while biodiesel produced from APSO with thermal activated catalyst is the single-output. The ANN architectural neural network in Figure 1 was designed to train 70% of the data of the process variables, validate 15% of the variables, and test 15% using the Levenberg-Marquardt training algorithm processed in the hidden layers with different neurons (10,17,20,23,30). The neuron with the least mean square error (MSE) was taken to be the best performing algorithm network, and the interactive effect of the process variable on the output was significant and maximized at data processed with the number of neurons. The best algorithm network was adopted to predict the optimal yield of biodiesel. This was done on a feed-forward back propagation network. The mean square error (MSE) is represented in Equation 3. The correlation coefficient (R^2) were determined.

$$MSE = \left(\sum_{i=1}^{n} \frac{(Predicted\ value - Experimental\ value)^2}{n}\right) \quad (3)$$

Where, *n* = number of datasets used to train the network

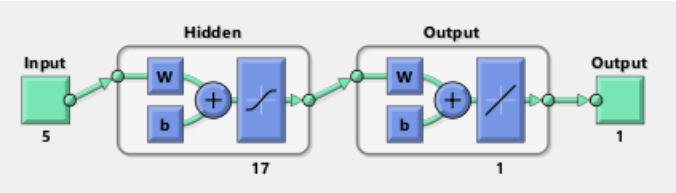

Fig. 1. ANN network architecture

Comment [h25]: No reference??

2.2.7 Characterization of biodiesel

The biodiesel produced at optimal conditions was characterized using a gas chromatography-mass spectrometer (GC-MS) and a fourier transform infra-red spectrometer (FTIR).

Comment [h26]: F

2.2.8 Sensitivity analysis of input variables

The impact of each process variable on the output in the MISO ANN model was ascertained using the connection weight model in MATLAB R2015a. The best processing neuron in the hidden layer having the least mean square error was used to process the data and train the network. The number of vertically connected weight layer from input and horizontally weight layer from output corresponds with the number of hidden neurons. The analysis algorithm is expressed as follows:

(a) Sum the vertically connected weights layer, $A_{ih,}$ for each input and determine their average.

$$A_{aih.} = \sum_{h=1}^{15}(\mathrm{Aih})/h \quad (4)$$

(b) Sum the horizontally connected weights layer for each output. $B_{toh} = \sum_{h=1}^{15}(Boh)$ (5)

(c) Multiply A_{aih} and B_{toh} using matrix multiplication method;

$C_{AB} = [A_{aih1}\ A_{aih2}\ \ldots\ A_{aih5}]\ [B_{toh1}]$ (7)

(d) Evaluate $D_{io} = \sum C_{AB}\ /n$ (8)

(e) Absolute value of $E_{io} = /A_{aih} - D_{io}/$ (9)

(f) Evaluate $F_{io} = \sum /A_{aih} - D_{io}/$ (10)

(g) The relative impact (RI) in percentage G_{io}= RI(%) $= \frac{Eio}{Fio}\ x\ 100$ (11)

3. RESULTS AND DISCUSSION

3.1 Properties of Africa Pear Seed Oil

The physiochemical properties of the Africa pear seed oil (APSO) are presented in Table 1. The oil has less free fatty acid which could be catalyzed by homogeneous and hetereogenous catalysts and does not require any form of pretreatment prior to transesterification. The magnitude of other properties like viscosity and energy value could be compared favourably with other non-edible oils such as *prunus amygdalus* [22], lard oil [23] and avocado seed oil [24]. Some of the Physiochemical properties of the APSO in this research are in agreement with Ofoefule [25].

Comment [h27]: P

Table 1: The summary of characterization of Africa pear seed oil

Properties	Africa pear seed oil
Specific gravity	0.9195
Kinematic viscosity(centistoke) at 40^0C	6.42
Refractive index	1.4715
Energy value (J/g)	30164
Flash point (^{o}C)	176
Fire point (^{o}C)	198
Acid value(mgKOH/kg)	5.01
Saponification value(mgKOH/kg oil)	135.26
Free fatty acid value(mgKOH/kg)	2.505
Peroxide value (meq/kg)	2.7421
Moisture content (%)	0.44
Molecular weight (g/mol)	880.87
Ester value (%)	94.46
Iodine value (mg I_2/100g oil)	25.13

3.2 Properties Of Raw and Modified Catalyst

The physiochemical properties, thermal properties, and structure of raw and thermally activated catalyst were determined using ASTM, BET, FTIR, SEM, and XRD analytical method/tools.

3.2.1 Catalysts characterization

The properties of the raw catalyst change when subjected to heat, as shown in Table 2. The ASTM analytical method was adopted to characterize the raw and activated EPFBA. The difference between the two catalysts was an indication of the effect of thermal activation, which is evident in high pore volume, low density, and low pore diameter.

Table 2. Properties of Catalysts by ASTM analysis

Sample/Properties	Raw EPFBA	Modified EPFBA
Conductivity	2.74	114.8
Ash(%)	6.08	34.48
Bulk density(g cm^{-3})	0.8147	0.6541
Organic carbon (%)	0.26	0.2
Organic matter (%)	0.80	0.59
Fixed carbon (%)	53.60	47.81
Volatile matter (%)	39.93	17.71
Particle density(g cm^{-3})	1.0030	1.0024
Total porosity (%)	18.77	34.78
Moisture (%)	-	-

3.2.2 BET analysis of the catalysts

The Brunauer-Emmet-Teller (BET) analysis in Table 3 confirms the ASTM characterization of the two catalysts when the two catalysts are compared. The activated catalyst (TAEPFBA) has more pore volume and surface area than the raw EPFBA. Moreso, the TAEPFBA requires less adsorption energy to adsorb the reactants. This is as a result of the presence of more pores compared to raw EPFBA.

Comment [h28]: ed

Comment [h29]: was

Table 3. BET analysis of different catalysts

Catalyst	Surface area (m^2/g)	Pore-volume (cc/g)	Pore-diameter (nm)	Adsorption energy(kJ/mol)
Raw EPFBA	173.955	0.108	2.144	4.530
Activated EPFBA	210.528	0.117	2.133	4.165

3.2.3 Fourier transform infrared (FTIR) analysis of the catalysts

The FTIR analytical technique was used to determine the functional group. The raw catalyst and activated catalyst have a wave number of 1028.7cm^{-1} and 1006.7cm^{-1}, respectively, confirming the presence of SiO_2 dominant around 1000cm^{-1} as shown in Figure 2a and 2b. The Si-O-Si bond was confirmed at a transmittance of 58 and 79 for raw and thermally treated catalyst. The spectra show the OH functional group at a wave number of 3257cm^{-1} and 3552.6cm^{-1} for raw and thermally modified EPFBA respectively, and at a transmittance of 82 and 90 respectively. The presence of OH and SiO_2 and having the alkali properties makes the catalyst a potential feedstock in the production of biodiesel via transesterification.

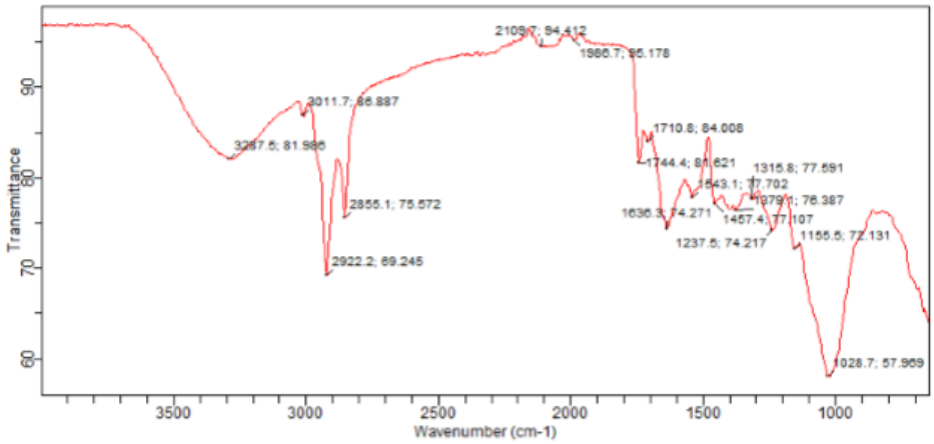

Fig 2a. FTIR spectrum of raw EPFBA

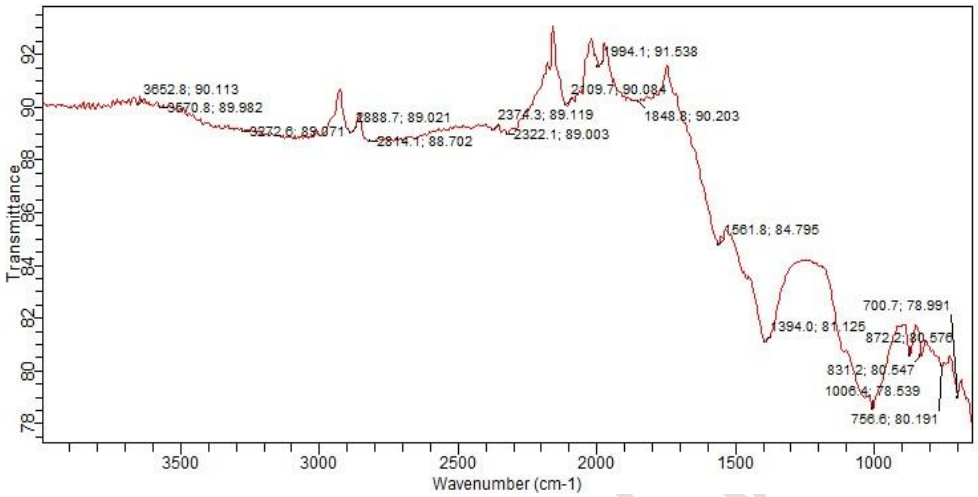

Fig 2b. FTIR spectrum of thermally modified EPFBA.

3.2.4 Scanning electron microscopes (SEM) of the catalysts

The morphology of the raw catalyst and TAEPFBA catalyst was investigated using the SEM analytical tool. The two catalysts were scanned with an electron microscope at a magnification of 300x and the pore sizes of the two catalysts were 889µm and 885µm for raw and activated catalysts, respectively, as shown in Figure 3a and Figure 3b. The result is similar to the analysis carried out using BET, with the thermally modified EPFBA having smaller pore sizes and a greater number of pores and surface area when compared to the raw catalyst. The catalyst's surface area and pore volumes allow for greater internal diffusion of reactant molecules.

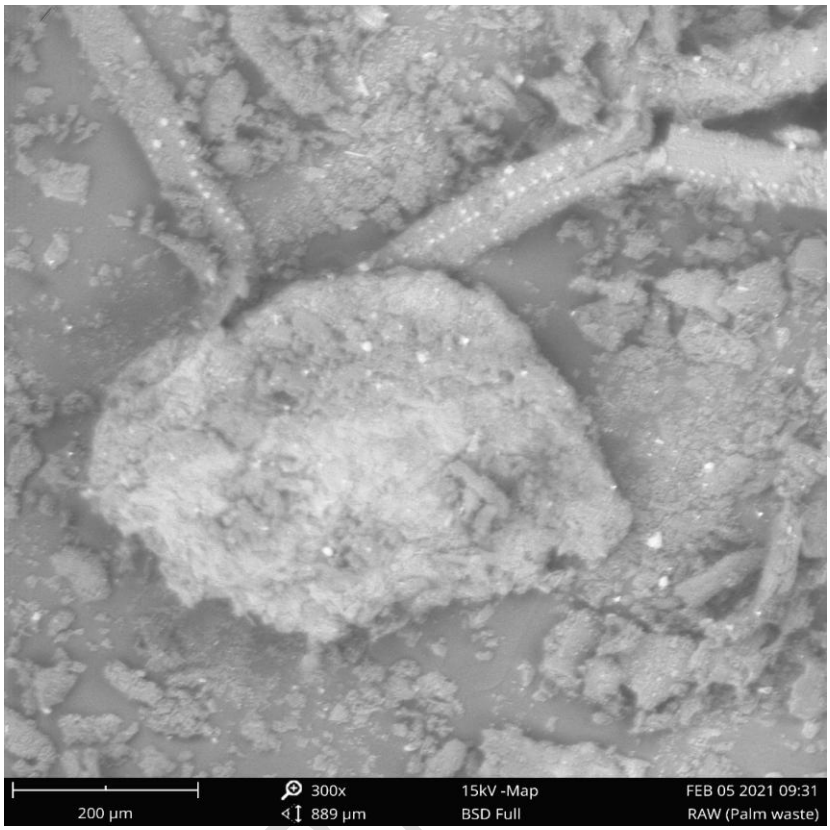

Fig. 3a. SEM for raw EPFBA catalyst at 300x magnification.

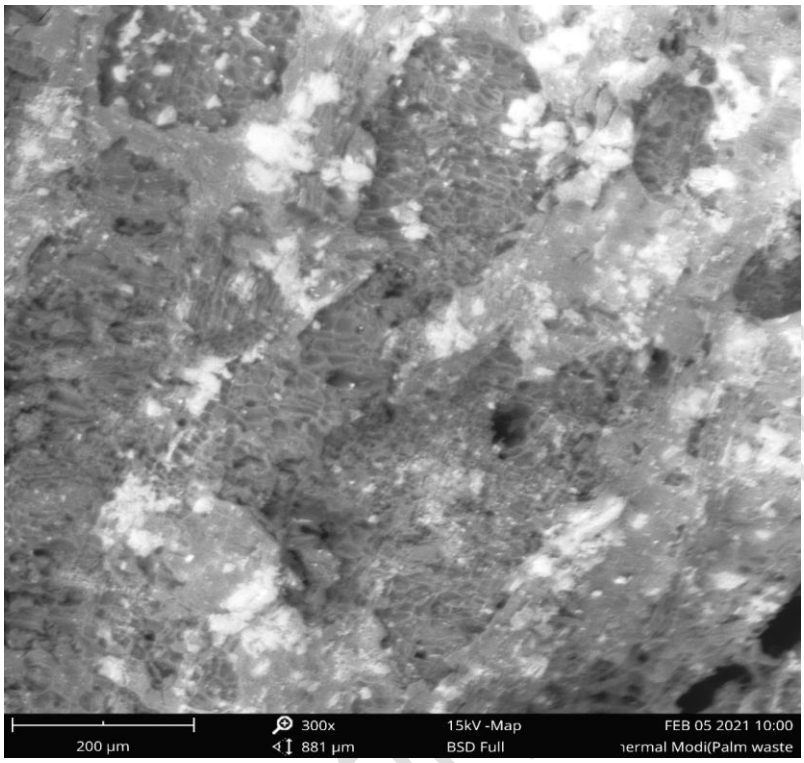

Fig. 3b. SEM for thermally activated EPFBA catalyst at 300x magnification.

3.3 Effect Of Process Variables on Biodiesel Yield

The effect of each process variable on the yield of biodiesel as it changes in magnitude was experimented with. This was achieved by varying one process parameter while the other variables were kept constant. The constant values of the process parameters for catalyst, methanol/oil ratio, temperature, reaction time, and agitation speed are 3wt %, 10:1, 60^{o}C, 3hrs, and 300 rpm, respectively.

3.3.1 Catalyst effect on biodiesel yield

The yield of alkyl ester increased as the catalyst weight percentage increased for both catalysts and then decreased as the catalyst (wt %) was increased beyond 3 wt.% as presented in Figure 4. This is as a result of insufficient reactants molecules needed to completely diffuse (mass transfer) into the pores of

the catalyst and, as a result, inhibit the contact between the reactants. Figure 4 shows that the yield of alkyl ester using TAEPFBA is significantly higher compared to the raw catalyst. This is attributed to having a large surface area and pores.

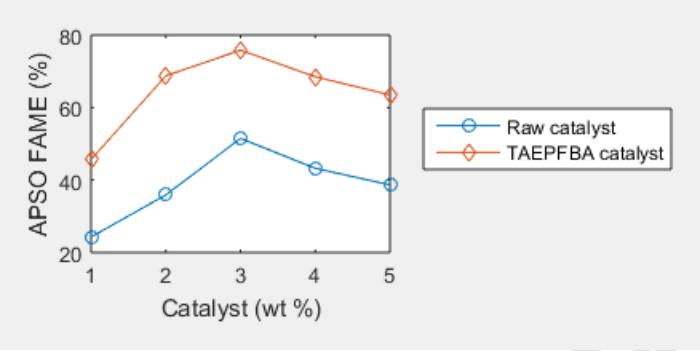

Fig 4. Effect of catalyst on FAME yield

3.3.2 Methanol/oil ratio effect on biodiesel yield

The yield of methyl ester to the different molar ratios indicated that methanol/oil molar ratio has a significant impact on biodiesel yield, as shown in Figure 5. The maximum methyl ester yield was obtained at a methanol/oil molar ratio of 10:1 for the raw EPFBA and activated EPFBA. The yield reduced when the molar ratio was higher than 10:1. The reason may be that the catalyst is insufficient to completely catalyze the methanol and oil as they increase in volume and, hence, may lead to little formation of ester. The results obtained are in line with the reports of earlier works by Ude and Onukwuli [26].

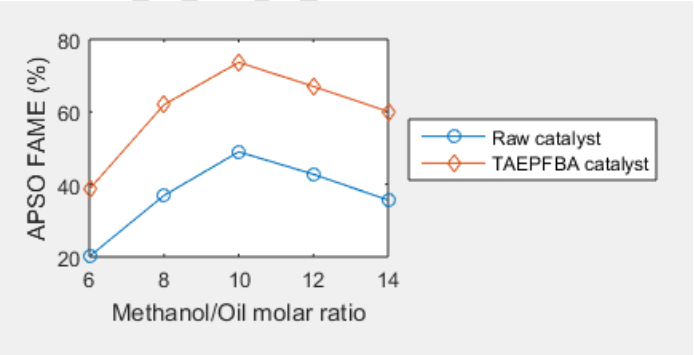

Fig 5. Effect of methanol/oil molar ratio on FAME

3.3.3 Effect of temperature on biodiesel Yield

The plot of temperature as it affects the yield of alkyl ester as shown in Figure 6 reveals that the optimal yield of biodiesel from APSO using raw and thermally activated catalyst is achievable at a temperature of 60^{o}C in a period of 3 hrs and at a speed of 300 rpm. Further increases in reaction optimal temperature, as shown in Figure 6, decreased the yield of biodiesel. This was attributed to the loss of methanol via vapourization since methanol's boiling point is below 66^{o}C. Similar result was reported by Hoque *et al.* [27]. The results also recommended that EPFBA modified gave a higher yield of biodiesel.

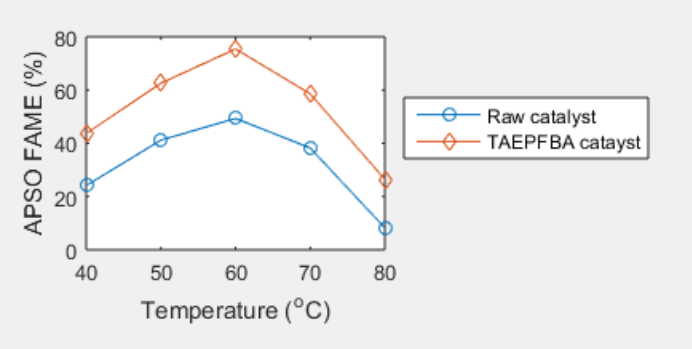

Fig. 6. Effect of temperature on biodiesel yield

3.3.4 Effect of time on biodiesel yield

The plot in Figure 7 shows that there was a significant difference between the yield of alkyl ester produced from APSO catalyzed with raw and TAEPFBA. This is in agreement with the result of Ude and Onukwuli (2019) that the yield of biodiesel increased as the clay (catalyst) was activated with alkaline. The effect of reaction time on biodiesel yield when using heterogeneous catalysts was ascertained and shown in Figure 7. It was discovered that the optimal reaction time was 3 hrs and beyond that, the yield decreased. The decrease is due to a reversible reaction of transesterification resulting in the loss of esters.

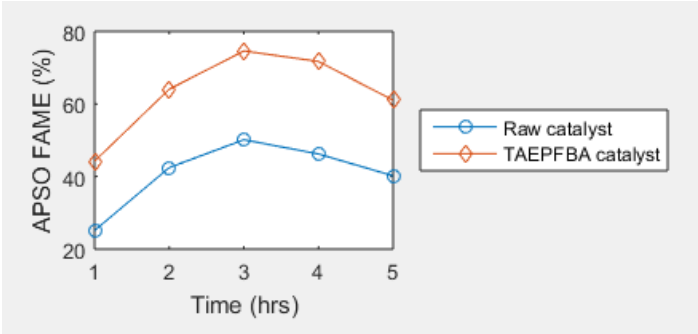

Fig. 7. Effect of time on APSO FAME yield

3.3.5 Effect of stirring speed on biodiesel yield

The collision between reactants and catalyst can be promoted and more effective if the reaction is agitated with a stirrer. The yield of methyl esters at different rates of mixing is shown in Figure 8. It was observed that the methanolysis reaction was practically complete at 300 rpm. The yield was observed to decrease as the stirring rate went above 300 rpm for raw EPFBA and modified EPFBA. This may be attributed to increase in pressure affecting the adsorption process, leading to soap formation. These results are in conformity with observations made by Chozhavendhan *et al.* [28].

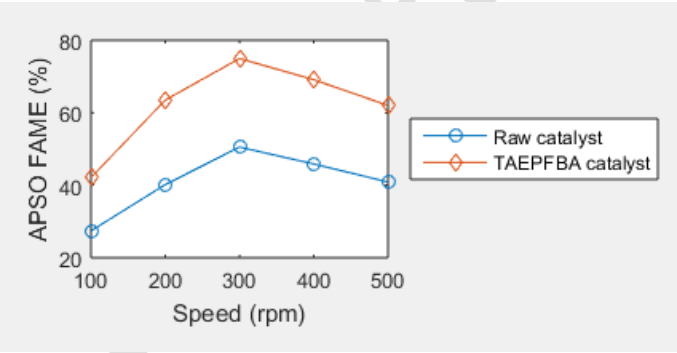

Fig. 8. Effect of speed on APSO FAME yield

3.4 Properties of biodiesel

The physio-chemical and thermal properties of biodiesel presented in Table 4 show that biodiesel has the potential to be run in diesel engines and also when blended with diesel. The results show that the

Comment [h30]: produced biodiesel

biodiesel produced has a higher cetane number than diesel, and Ude et al. (2021) obtained a similar result using Africa pear seed oil and clay as catalysts. The high cetane number is as a result of high oxidative stability and chemical activity with a low caloric value. The biodiesel advantage over diesel can be traced to variables like density, cetane number, and combustion. Biodiesel burns completely longer than diesel because of the oxygen content, making it a better lubricant. In addition, biodiesel is sulfur free and is one of the reasons diesel engines emit fewer toxic substances when operated with biodiesel.

Table 4. Properties of Biodiesel and its Blends produced from Africa pear seed oil

Parameters	B_0	B_{20}	B_{40}	B_{60}	B_{80}	B_{100}
Viscosity@40^oC (mm^2/s)	1.189	1.270	1.908	2.092	2.871	3.577
Density (g/cm^3)	0.8283	0.8600	0.8712	0.8797	0.8897	0.8948
Flash point (^oC)	56.00	96.00	103.00	121.00	139.00	171.00
Fire point (^oC)	78.00	115.00	123.00	145.00	159.00	194.00
Cloud point (^oC)	4.00	4.50	6.00	7.50	9.00	10.00
Pour point (^oC)	2.00	2.50	3.50	4.50	5.00	6.00
Acid value (mg KOH/g)	-	0.02	0.034	0.04	0.044	0.050
Freefattyacid(mgKOH/g)	-	0.01	0.017	0.02	0.022	0.025
Aniline Point (^oC)	58.50	54.60	52.50	46.50	38.50	36.00
Diesel index	54.08	45.18	39.96	34.68	28.91	25.64
API Gravity	39.33	34.97	32.05	30.45	28.04	26.99
Cetane Number	53.55	57.48	64.98	68.89	71.91	73.94
Gross calorific value (J/g)	47074	46753	46491	46474	45823	45722

3.5 GS-MS Result of Biodiesel

Comment [h31]: delete

The methanolysis conversion of fatty acid of APSO catalysed with TAEPFBA to alkyl ester is presented in Figure 9. From the Figure, it is observed that the triglyceride was converted to methyl esters. The highest peaks indicate the presence of methyl esters, while the lower peaks on the right hand side indicate the presence of monoglyceride, diglyceride and unconverted triglyceride.

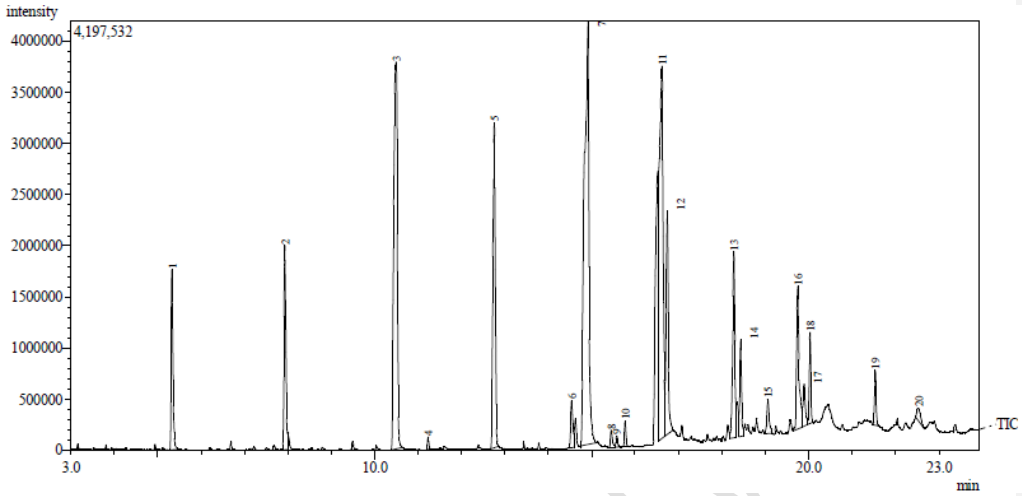

Fig. 9. GC-MS of APSO FAME produced by TAEPFBA catalyzed reaction at optimal condition

Comment [h32]: delete

3.6 FTIR Characterization of Biodiesel

Figure 10 shows the fourier transform infra-red spectrum for the conversion of triglyceride of APSO to methyl ester by TAEPFBA. From the Figure, the IR peak at 3050-3900 cm-1 is attributed to the stretching of hydroxyl (OH) groups in the biodiesel. The IR peaks at 1300–1600 cm^{-1} are assigned to the peaks of bending vibration of O=C=O group. The two bands within the range of 2100–2890 cm^{-1} and peak at 1750 cm-1 on the IR spectra are ascribed to the C-H stretching of the alkyl group and the C=O stretching of the esters group, respectively. These bands occurred because of the unconverted triglyceride in the oils.

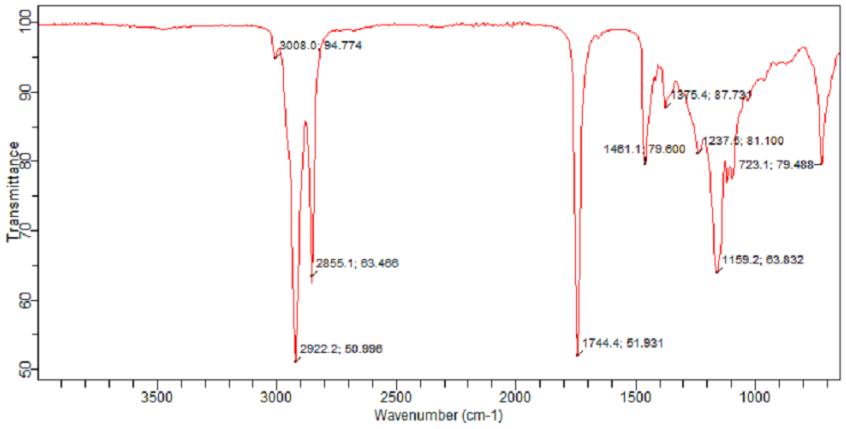

Fig. 10. FTIR of APSO FAME produced by TAEPFBA catalyzed reaction at optimal conditions.

3.10 Prediction of APSO FAME Yield Using ANN model

Comment [h33]: y

Comment [h34]: u

Table 5 shows that seventeen (neurons) in the hidden layer of the ANN neural network could effectively train the input data and maximize the data for maximum output. Hence, the number of neurons was used to predict the output. Figures 11, 12, and 13 depict the error performance plot, error histogram, and regression plot respectively, of the seventeen training, validating, and testing neurons. As seen in Figure 11, the MSE dropped from 1000 to 0.021365 at epoch 5. The training and testing of process variables were significantly achieved at epoch 5 at the best performance validation. The maximum number of epochs for performing the best validation was 6. The error histogram as shown in Figure 12 shows that the errors fall between -0.01822 and 0.1258 (zero region), indicating a good performance. Figure 13 shows the best fit between the target data and the output data. The correlation coefficient indicates that the best training, testing, and validation were carried out using the MISO architectural neural network with seventeen neurons.

Table 6 shows the predicted yield of APSO FAME using the ANN model. The percentage errors between the experimental yield and the predicted optimal yield of APSO FAME with ANN model is 0.02% . The statistical indices confirm that the model can be used to predict the yield of biodiesel.

Table 5. The MSE best performance and correlation coefficient

Number of neuron	MSE	Epoch	R
10	0.1324	6	0.9972
17	0.0214	5	0.9977
20	0.2320	5	0.9977
23	0.0316	3	0.9672
30	0.0465	5	0.9968

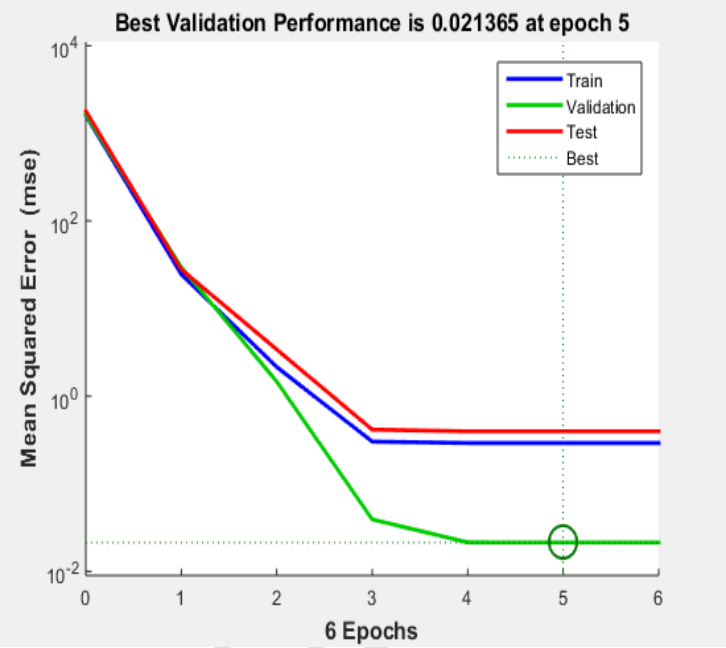

Fig 11. Validation performance error curve using seventeen neurons network

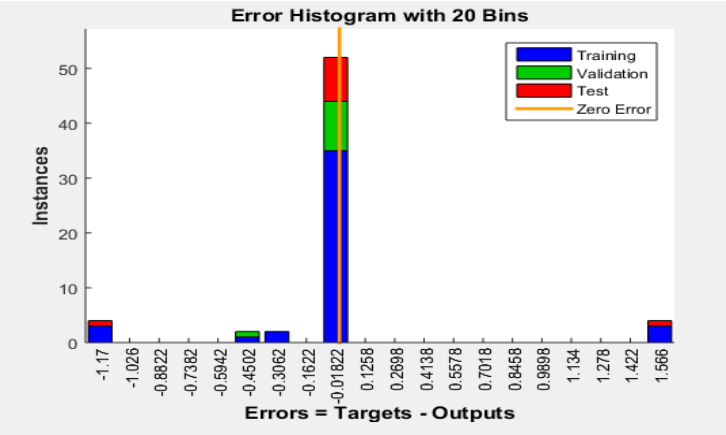

Fig 12. Error Histogram of experimented data and predicted data on MISO ANN model

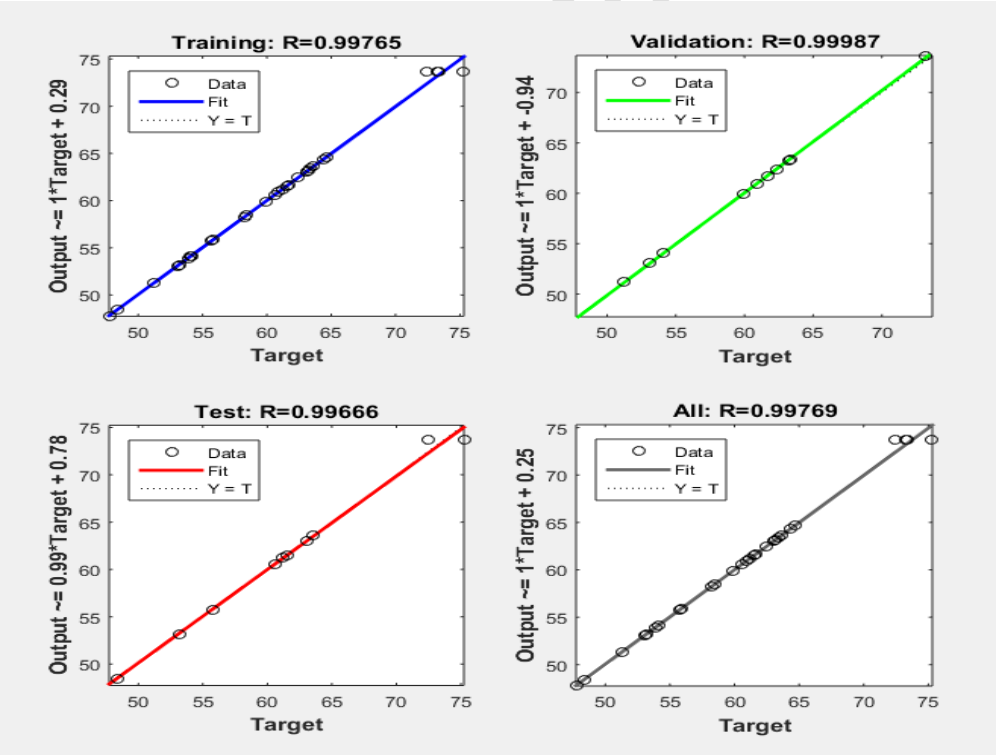

Fig. 13. ANN Regression plot analysis using seventeen neurons.

Table 6: Actual and predicted responses of APSO transesterification process using TAEPFBA catalyst

Run order	Catalyst conc. (wt %) A	Methanol/ Oil molar ratio B	Temperature (^{o}C) C	Time (hrs) D	Agitation Speed (Rpm) E	Biodiesel yield from carbonized catalyst (vol. %)	Biodiesel yield by TAEPFBA (vol. %) ANN
1	2	8	50	2	400	53.17	54.14
2	4	8	50	2	200	47.74	43.96
3	2	12	50	2	200	54.11	54.36
4	4	12	50	2	400	58.24	54.04
5	2	8	70	2	200	48.43	44.94
6	4	8	70	2	400	61.66	64.11
7	2	12	70	2	400	61.53	52.91
8	4	12	70	2	200	53.9	56.70
9	2	8	50	4	200	53.1	45.00
10	4	8	50	4	400	55.74	64.09
11	2	12	50	4	400	63.2	51.12
12	4	12	50	4	200	60.88	61.37
13	2	8	70	4	400	59.92	57.56
14	4	8	70	4	200	54.09	55.06
15	2	12	70	4	200	58.46	70.39
16	4	12	70	4	400	64.39	56.20
17	1	10	60	3	300	61.22	64.76
18	5	10	60	3	300	62.41	54.18
19	3	6	60	3	300	53.16	59.12
20	3	14	60	3	300	63.37	61.95
21	3	10	40	3	300	60.59	54.03
22	3	10	80	3	300	64.64	61.87
23	3	10	60	1	300	55.84	54.00
24	3	10	60	5	300	63.59	51.21
25	3	10	60	3	100	51.27	44.36
26	3	10	60	3	500	63.06	64.75
27	3	10	60	3	300	75.23	75.38
28	3	10	60	3	300	73.35	75.38
29	3	10	60	3	300	75.31	75.38
30	3	10	60	3	300	72.43	75.38
31	3	10	60	3	300	73.21	75.38
32	3	10	60	3	300	72.43	75.38

Table 7. Model Summary Statistics and predicted APSO FAME yield

Model (APSOFAME)	% error	MSE	R^2	APSO FAME (%)
ANN model	0.20	0.0214	0.9977	75.38

3.11 Sensitivity Analysis Of Input Variables

The relative contribution of process parameters to the output train on the MISO ANN architectural network with 17 hidden neurons is presented in Figure 14. The Figure shows that the temperature has the

greatest contribution (40.7%). However, the methanol/oil ratio shows a small percentage contribution of less than 15%, and this is reflected in the RSM model, with the methanol/oil ratio having the highest negative coefficient and antagonistic interaction with other variables.

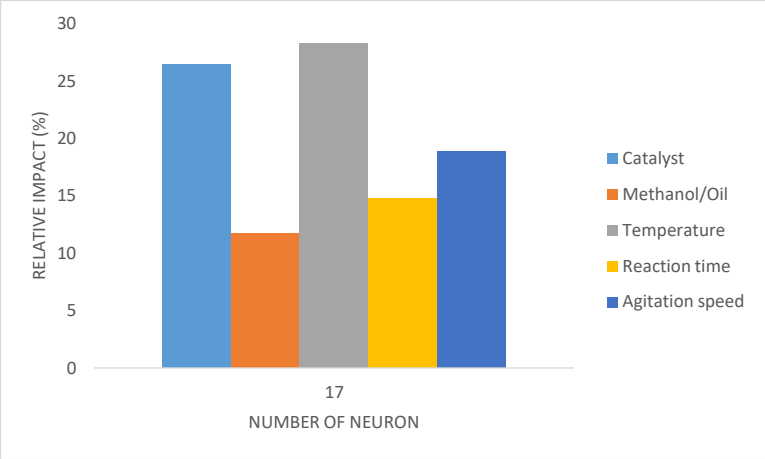

Fig. 14. Contribution of transesterification process variables in APSO FAME yield

Comment [h35]: delete

4. CONCLUSION

The production of biodiesel at optimal conditions from Africa pear seed oil using heterogeneous catalyst TAEPFBA, validation of the ANN model equation via process variables and the relative impact of the various process parameters were carried out. The transesterification method was adopted without treating the oil. The transesterification results show the yield of methyl ester increased significantly after the EPFBA had been thermally activated. This is an indication that it is pertinent to calcine the catalyst (EPFBA) at 800^{o}C. The process variables are relevant in biodiesel production, which was ascertained from the ANN equation analysis. Optimization of the reaction parameters for biodiesel production from Africa pear seed oil was carried out using ANN tools. Their predicted values certified the techniques to be recommended for predicting the biodiesel yield. The optimal values of the parameters were: catalyst concentration of 3wt%, methanol/oil ratio of 10:1, temperature of 60^{o}C, time of 3 hrs, and reaction speed of 300 rpm. The percentage yield of biodiesel from APSO oil using TAEPFBA shows that the catalyst has the potential to be used as a catalyst to transesterify edible and non edible oils to biodiesel. The sensitivity analysis carried out shows that the temperature has the highest relative impact and the methanol/oil ratio has the least relative contribution. The physiochemical properties of biodiesel produced under optimized conditions meet the ASTM standard and are within the recommended limits.

Comment [h36]: delete

Comment [h37]: Are sure of this hightemperature?

Comment [h38]: 3 wt. %

CONSENT FOR PUBLICATION

All the authors gave their consent for the publication.

REFERENCES

1. Lee JH, Kim SB, Kang SW, Song YS, Park C, Han SO, and Kim SW. Biodiesel production by a mixture of Candida rugosa and Rhizopus oryzae lipases using a supercritical carbon dioxide process. Bioresource technology. 2011;102(2):2105-2108. https://doi.org/10.1016/j.biortech.2010.08.034
2. Ude CN, Onukwuli OD, Okey-Onyesolu FC, Nnaji PC, Okoye CC and Uwaleke CC. Heterogeneous Catalysis of African Pear Seed Oil and Modelling of Some Thermo-Physical Properties of its Biodiesel. Research square. 2021
3. Umeuzuegbu JC, Okiy S, Nwobi-Okoye CC, and Onukwuli OD. Computational modeling and multi-objective optimization of engine performance of biodiesel made with castor oil. Heliyon. 2021;7(3). https://doi.org/10.1016/j.heliyon.2021.e06516
4. Ude CN, Onukwuli OD, Nwobi-okoye C, Anisiji OE, Atuanya CU, and Menkiti MC. Performance evaluation of cottonseed oil methyl esters produced using CaO and prediction with an artificial neural network. Biofuels. 2020 https://doi.org/10.1080/17597269.2017.1345355
5. Szulczyk KR and McCarl BA. Market penetration of biodiesel. Renewable and Sustainable Energy Reviews. 2010;14(8): 2426-2433. https://doi.org/10.1016/j.rser.2010.05.008
6. Ofoefule AU, Ibeto CN, Okoro UC and Onukwuli OD. Biodiesel production from tigernut (Cyperus esculentus) oil and characterization of its blend with petro-diesel. Physical Review & Research International. 2013;3(2): 145-153
7. Onukwuli OD, Emembolu LN, Ude CN, Aliozo SO, and Menkiti MC. Optimization of biodiesel production from refined cotton seed oil and its characterization. Egyptian Journal of Petroleum. 2017;16(1):103-110. https://doi.org/10.1016/j.ejpe.2016.02.001
8. Paula RS, Figueredo IM, Vieira RS, Nascimento TL, Cavalcante CL, Machado YL and Rios MA. Castor–babassu biodiesel blends: estimating kinetic parameters by Differential Scanning Calorimetry using the Borchardt and Daniels method. SN Applied Sciences. 2019;1(8): 1-7.
9. Antony MG, Bose N and Edwin RR. Optimization of process parameters for biodiesel extraction from tamanu oil using design of experiments. Journal of Renewable and Sustainable Energy. 2014;6(3):033120. https://doi.org/10.1063/1.4880216
10. Jose DM, Raj RE, Prasad BD, Kennedy ZR, and Ibrahim AM. A multi-variant approach to optimize process parameters for biodiesel extraction from rubber seed oil. Applied Energy. 2011;88(6):2056-2063.
11. Kumar K, Singh J, Nanoti SM and Garg MO. A comprehensive life cycle assessment (LCA) of Jatropha biodiesel production in India. Bioresource Technology. 2012;110:723-729. https://doi.org/10.1016/j.biortech.2012.01.142
12. Anyanwu CN, Mbajiorgu CC, Ibeto CN and Ejikeme PM. Effect of reaction temperature and time on neem methyl ester yield in a batch reactor. Energy conversion and management. 2013;74:81-87. https://doi.org/10.1016/j.enconman.2013.04.029
13. Godugula V and Srinivas I. The ethanolosis of *pongamia pinnata* oil by a two-stage acid-base catalyst transesterification process for production of biodiesel. Energy Sources, Part A: Recovery, Utilization, and Environmental Effects. 2012;34(16):1550-1558.

Comment [h39]: Ensure all the in-text references are cited and written according to the guidelines

Comment [h40]: italise

Comment [h41]: italise, no pages??

Comment [h42]: italise

Comment [h43]: italise

Comment [h44]: italise

Comment [h45]: italise

Comment [h46]: italise

Comment [h47]: italise

Comment [h48]: italise

Comment [h49]: italise

Comment [h50]: italise

Comment [h51]: italise

14. Onoji SE, Iyuke SE, Igbafe AI and Nkazi DB. Rubber seed oil: A potential renewable source of biodiesel for sustainable development in sub-Saharan Africa. Energy conversion and management. 2016;110: 125-134. https://doi.org/10.1016/j.enconman.2015.12.002

15. Sundar K and Udayakumar R. Comparative evaluation of the performance of rice bran and cotton seed biodiesel blends in VCR diesel engine. italise. 2020;6:795-801. https://doi.org/10.1016/j.egyr.2019.12.005

16. Onukwuli OD, and Ude CN. Kinetics of African pear seed oil (APO) methanolysis catalyzed by phosphoric acid-activated kaolin clay. Applied Petrochemical Research. 2018; 8(4): 299-313.

17. Iloamaeke IN, Onuigbo CC, Umedum IN, Umeobika CU, and Oforah PU. Production and characterization of biodiesel from the seed of Dacryodes edulis (African pear). Int. J. Curr. Res. 2016; 8: 25230-25234.

18. Isong AU, Davies AU, Elechi O, and Effiong EI. Biodiesel Synthesis from African Pear (Dacryodes edulis) Oil Using Catalyst Assisted Transesterification Process. World. 2020;5(4):65-69.

19. Bull OS and George DM. Assessment of fuel properties of biodiesel obtained from African Pear (Dyacrodes edulis) seeds oil. italise. 2015;2(10): 894-898.

20. Zabeti M, Daud WM and Aroua MK. Biodiesel production using alumina-supported calcium oxide: An optimization study. Fuel processing technology. 2010;91(2):243-248. https://doi.org/10.1016/j.fuproc.2009.10.004.

21. Zahira Y, Irwan SBS, Binitha N, Siti RSA and Manal I. Utilization of palm empty fruit bunch for the production of biodiesel from Jatropha curcas oil. Bioresource Technology. 2011;10(4): 695–700.

22. Esonye, C, Onukwuli OD, and Ofoefule AU. (2019). Optimization of methyl ester production from Prunus Amygdalus seed oil using response surface methodology and Artificial Neural Networks. Renewable energy. 2019;130: 61-72. https://doi.org/10.1016/j.renene.2018.06.036

23. Ezekannagha CB, Ude CN and Onukwuli OD. Optimization of the methanolysis of lard oil in the production of biodiesel with response surface methodology. Egyptian Journal of Petroleum. 2017;26(4):1001-1011. https://doi.org/10.1016/j.ejpe.2016.12.004

24. Viswanathan K, Taipabu MI, Wu W and Wang S.. A comprehensive investigation on the effects of ceramic layering and cetane improver with an avocado seed oil biodiesel fueled diesel engine. Bioenergy Resources and Technologies. 2021; 293-332.

25. Ofoefule AU, Esonye C, Onukwuli OD, Nwaeze E and Ume CS. Modeling and optimization of African pear seed oil esterification and transesterification using artificial neural network and response surface methodology comparative analysis. Industrial Crops and products. 2019140(5),111707. https://doi.org/10.1016/j.indcrop.2019.111707

26. Ude CN and Onukwuli OD. Kinetic modeling of transesterification of gmelina seed oil catalyzed by alkaline activated clay (NaOH /clay) catalyst. *Reaction Kinetics, Mechanisms and Catalysis.* 2019;*127*(2): 1039-1058. https://doi.org/10.1007/s11144-019-01604-x

27. Hoque MN, Singh A and Chuan YL.. Biodiesel from low cost feedstocks: The effects of process parameters on the biodiesel yield. Biomass and Bioenergy. 201135(4): 1582-1587. https://doi.org/10.1016/j.biombioe.2010.12.024

28. Chozhavendhan, S., Singh MVP, Fransila, B, Kumar RPI, and Devi GK. (2020). A review on influencing parameters of biodiesel production and purification processes. *Current Research in Green and Sustainable Chemistry*, *1*, 1-6. https://doi.org/10.1016/j.crgsc.2020.04.002

Comment [h52]: italise

Comment [h53]: italise

Comment [h54]: italise

Comment [h55]: italise

Comment [h56]: italise

Comment [h57]: italise

Comment [h58]: italise

Comment [h59]: italise